Tissue-Specific Distribution and Bioaccumulation of Perfluoroalkyl Acids, Isomers, Alternatives and Precursors in Citrus Trees of Contaminated Fields: Implication for Risk Assessment

Zhaoyang Liu [a, *, 1], Shun Liu [b, 1], Feng Xiao [c], Andrew J. Sweetman [d], Xiang Wan [a, e], Mingxia Wang [a], Chang Chen [a], Hao Guo [a], Ziyao Luo [a], Linlin Zhong [f], Jay Gan [g], Wenfeng Tan [a]

[a] *State Environmental Protection Key Laboratory of Soil Health and Green Remediation, College of Resources and Environment, Huazhong Agricultural University, Wuhan 430070, China*

[b] *The Seventh Geological Brigade of Hubei Geological Bureau, Yichang 443100, China*

[c] *Department of Civil and Environmental Engineering, University of Missouri, Columbia, MO 65211, USA*

[d] *Lancaster Environment Centre, Lancaster University, Lancaster LA1 4YQ, UK*

[e] *Hubei Geological Survey, Wuhan 430034, China*

[f] *National Key Laboratory for Germplasm Innovation & Utilization of Horticultural Crops, Huazhong Agricultural University, Wuhan 430070, China*

[g] *Department of Environmental Sciences, University of California, Riverside, CA 92521, USA*

*Corresponding author: Zhaoyang Liu, Tel: 86-27-87287508, Fax: +86-27-87288618, E-mail: zhaoyangliu@mail.hzau.edu.cn

[1] Zhaoyang Liu and Shun Liu are the co-first authors of this article.

Abstract: The ingestion of fruits tainted with perfluoroalkyl acids (PFAAs) presents potential health hazards. This study aimed to fill knowledge gaps about the distribution

patterns and bioaccumulation behaviors of PFAAs, isomers, alternatives, and precursors (collectively as per- and polyfluoroalkyl substances, PFAS) within different tissues of citrus trees grown in contaminated fields and further highlighted the contribution of precursor degradation to exposure risks. Alarming concentrations of total target PFAS ($\sum PFAS_{target}$, 92.5–7496 ng/g dw) and unknown precursors measured through oxidation (131–13979 ng/g dw) were found in citrus tree tissues. Short-chain PFAS constituted primary components in citrus trees, and total PFAS concentrations followed the order of leaves > fruits > branches, barks > woods, and peels > pulps > seeds. PFAS levels in barks and woods rose with diminishing branch diameters. The average contamination burden of peels ($\sum PFAS_{target}$: 57.7%; unknown precursors: 71.2%) was highest in fruits. The translocation potential and bioaccumulation factor (BAF) of short-chain, branched, or carboxylic acid-based PFAS exceeded those of their relatively hydrophobic counterparts, and ether bond-based PFAS showed lower BAFs than similar PFAAs in citrus trees. In the risk assessment of consuming contaminated citruses by residents, precursor degradation approximately contributed 36% to total PFAS exposure, and should not be ignored.

Key words: PFAS; total oxidizable precursor (TOP) assay; citrus tree; bioaccumulation behavior; health risk

Environmental Implications: The consumption of fruits tainted with PFAS may pose potential health threats. The purpose of this study is to provide systematic insights into distribution patterns, relative burdens, translocation potentials and bioaccumulation specificities of PFAS of varying chain-lengths, isomeric structures, ether bonds and functional groups in different tissues of citrus trees. A TOP assay is innovatively introduced in the bioaccumulation analysis and risk assessment for unknown precursors. These new findings aid safety evaluation and risk mitigation of fruit planting in potential PFAS-polluted regions.

1. Introduction

Perfluoroalkyl acids (PFAAs) represent a broad category of widely-used anthropogenic chemicals that have garnered global concern due to their ubiquitous presence in the environment (Barzen-Hanson et al., 2017; Trang et al., 2022; Wang et al., 2015). Legacy long-chain PFAAs, such as perfluorooctane sulfonic acid (PFOS) and perfluorooctanoic acid (PFOA), have been of particular concern because of their detrimental effects on human health, including impacts on immunity, metabolism, endocrinology, reproduction, and fetal and postnatal growth (Chang et al., 2022; Greenhill, 2017; Zheng et al., 2021). As a result, these chemicals have been classified as emerging contaminants of significant concern in international restriction agreements, such as the Stockholm Convention (Evich et al., 2022; UN Environment Programme, 2020). In response to the expanding global market demands, efforts have been made to replace legacy long-chain PFAAs with shorter-chain homologs and a variety of perfluoroalkyl ether acids (PFEAs) (Lim, 2019; Wang et al., 2017; Xiao, 2017). However, growing evidence suggests that these substitutes may pose ecological and human health risks similar to those associated with legacy long-chain PFAAs (Gomis et al., 2018; Qin et al., 2022).

Due to their widespread use and environmental persistence, PFAAs have the potential to contaminate agricultural lands and, subsequently, the crops grown on these soils (Li et al., 2019; Liu et al., 2017). The consumption of contaminated fruits has been identified as an important pathway of exposure to PFAAs for humans (Pasecnaja et al., 2022; Sznajder-Katarzynska et al., 2018). Previous studies primarily focused on the

74 occurrence of PFAAs in fruit pulps (Klenow et al., 2013; Li et al., 2019), but less on
75 the tissue-specific distribution, translocation potentials, and bioaccumulation behaviors
76 of PFAAs in fruit trees, which are imperative for the safety evaluation of fruit planting
77 in contaminated soils.

78 Despite growing awareness of the potential health risks associated with PFAA
79 exposure, there remains limited information on the concentrations and accumulation of
80 PFAA isomers in fruits. PFAA production in China is mainly based on the
81 electrochemical fluorination (ECF) process, and generally yields a mixture of linear and
82 branched isomers (Schulz et al., 2020). As branched PFAAs may exhibit different
83 physicochemical properties from their linear isomers (Chen et al., 2015; Schulz et al.,
84 2020), their accumulation potentials in fruit planting could vary significantly, leading
85 to diverse exposure risks for humans. Studying isomer-specific bioaccumulation in fruit
86 trees contributes to obtaining a comprehensive understanding of the behavior and fate
87 of these chemicals in the environment.

88 PFEAs such as hexafluoropropylene oxide dimer acid (HFPO-DA, with the
89 trade name of GenX) were developed as novel alternatives of PFAAs by inserting one
90 or more ether bonds into the carbon chain, which may be more likely to accumulate in
91 animals and human beings (Cui et al., 2018; Wang et al., 2020a). For example, the
92 bioaccumulation capacity of GenX in the fish liver was about 3-fold higher than that of
93 perfluorohexanoic acid (PFHxA) with the same number of carbon atoms (Pan et al.,
94 2017). Hexafluoropropylene oxide trimer acid (HFPO-TA) is a new PFEA measured in
95 environmental samples (Pan et al., 2018). Nevertheless, to date, there have been few

reports about the effects of introduced ether bonds on the bioaccumulation of these emerging PFAS in different organs of fruit trees.

Furthermore, thousands of unknown precursors, which can be transformed into more persistent and potentially toxic PFAAs during chemical, biological and thermal processes (Xiao et al., 2012; Xiao et al., 2018; Xiao et al., 2021), present in multiple environmental matrices and living organisms (Jin et al., 2020; Munoz et al., 2020). However, limited information currently exists on the concentrations and accumulation of these precursors in plant tissues. A total oxidizable precursor (TOP) assay, which can oxidize precursors into quantifiable perfluoroalkyl carboxylic acids (PFCAs) (Houtz and Sedlak, 2012), can be used to indirectly study the distribution and bioaccumulation of unknown precursors in fruit trees. In addition, previous risk assessments were mainly based on target PFAAs in food, which ignored the potential degradation of precursors during digestion and other biochemical processes in human bodies and resulted in an underestimation of health risks (Diao et al., 2022; McDonough et al., 2022). Therefore, an improved approach to risk assessment considering precursor degradation is urgently called for a better protection for fruit consumers.

In general, the distribution patterns and bioaccumulation behaviors of PFAA-related chemicals in fruit trees are relatively under-studied. However, fruit dietary intakes may be particularly significant because most of them are consumed raw or with minimal processing. As a globally representative fruit, citrus is favored by a wide range of consumers. Taking citrus tree as an example, this study aimed to fill above-mentioned knowledge gaps and provide new insights into the translocation,

bioaccumulation and human exposure of PFAAs, isomers, alternatives and precursors (collectively designated as per- and polyfluoroalkyl substances, PFAS) in fruit trees of contaminated fields. Specific objectives include (i) determining the occurrence and distribution of PFAS in branches (barks and woods) with different diameters, leaves and fruits (peels, pulps and seeds) of citrus trees; (ii) identifying the influences of molecular structures (e.g., isomer, ether bond, carbon chain length and functional group) of individual PFAS, as well as the morphology and physiology of different tissues on translocation and bioaccumulation potentials of these chemicals in citrus trees; and (iii) estimating the potential contribution of unknown precursors to health risks of PFAS through citrus consumption and developing a risk assessment approach considering precursor degradation by TOP assay. This study represents the first instance in the literature of an investigation into the tissue-specific distribution and bioaccumulation of PFAS with varying chain lengths, isomeric structures, ether bonds, and functional groups, as well as unknown precursors in fruit trees. These findings have the potential to inform the development of effective risk management strategies aimed at maintaining food safety and preserving public health.

2. Materials and methods

2.1 Sampling design and collection

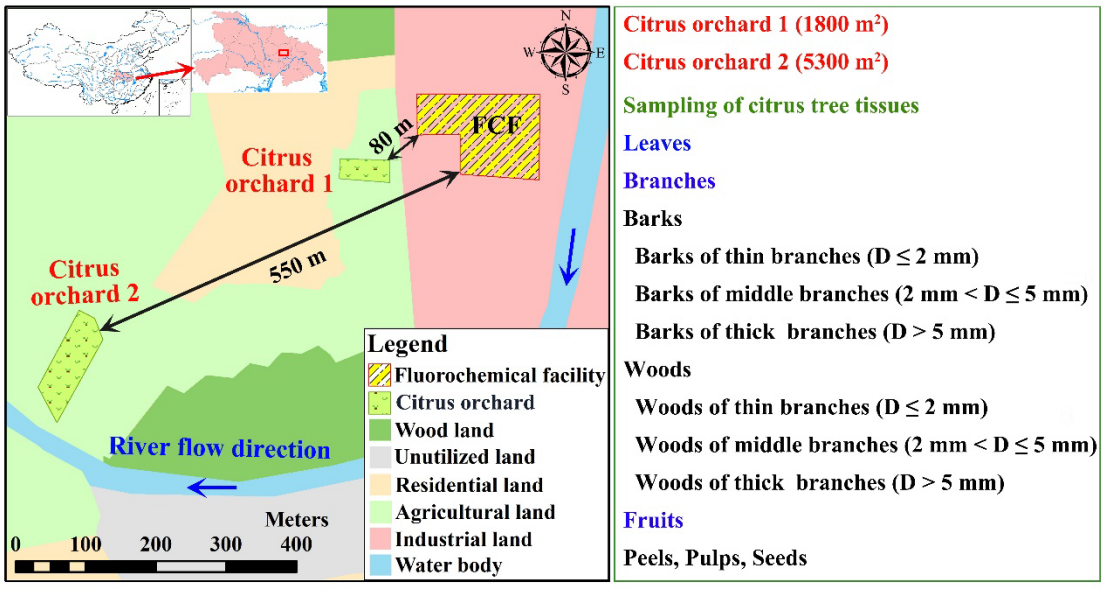

Fig. 1 Map of sampling locations for citrus tree tissues and corresponding soils near the fluorochemical facility (FCF) in Hubei Province, central China.

Note: "D" represents the branch diameters.

The study area was near a large fluorochemical facility (FCF) located in Hubei Province, central China. This facility has been producing C4-C8 PFAS through the ECF process since 2006 (seeing major products in SI 1.1). The study area comprises vast agricultural lands, with citrus being the primary local fruit crop. Two citrus orchards were selected for this study: "Orchard 1 (O1)" was situated adjacent to the FCF, covering an area of approximately 1800 m^2; and "Orchard 2 (O2)" was located around 550 m southwest of the FCF, spanning an area of roughly 5300 m^2 (Fig. 1). Site information and ambient conditions are presented in Table S1.

In December 2020, a substantial number of branches bearing leaves and mature fruits were cut from the citrus canopy at different heights (top, middle, bottom) and in

eight directions using pre-cleaned scissors. The scissors were pre-rinsed three times with ultra-pure water and three times with methanol before each use. Five sub-sites, consisting of the center and four corners of the orchard, were sampled, and each sub-site contained five citrus trees. The collected branches bearing leaves and mature fruits were then separated into branches, leaves and fruits, and individual samples of the same category from 25 citrus trees within a single orchard were amalgamated into a single composite sample. The plant samples were wrapped in aluminum foil and stored in clean paper bags. Moreover, the corresponding topsoil samples (0−20 cm) beneath each citrus tree at the five sub-sites were gathered and uniformly mixed. The sampling procedures for plants and soils were similar to the approaches previously described by Dick et al. (1997), Ryan et al. (1982), Eun et al. (2020) and Yamazaki et al. (2023) respectively, which were commonly used in environmental monitoring. Detailed information on the heights, ground diameters, and coverage of citrus trees are provided in Table S2. The sample lists and corresponding explanations can be found in Table S3. Furthermore, the standardized procedures for sample collection and transport are detailed in the Supporting Information (SI 1.1).

2.2 Standards and reagents

This study identified a total of 26 PFAAs and alternatives in all samples, including eleven PFCAs with carbon lengths from C4 to C14, seven perfluoroalkane sulfonic acids (PFSAs) with carbon lengths from C4 to C10 and eight novel alternatives such as GenX, ammonium 4,8-dioxa-3H-perfluorononanoate (ADONA) and HFPO-TA, which are the substitutes of PFCAs, as well as 6:2 chlorinated polyfluorinated ether

sulfonate (6:2 Cl-PFESA), 8:2 chlorinated polyfluorinated ether sulfonate (8:2 Cl-PFESA), 4:2 fluorotelomer sulfonate (4:2 FTS), 6:2 fluorotelomer sulfonate (6:2 FTS) and 8:2 fluorotelomer sulfonate (8:2 FTS), which can be used to replace PFSAs. In addition, five target precursors including perfluorobutanesulfonamide (FBSA), perfluorohexanesulfonamide (FHxSA), perfluorooctanesulfonamide (FOSA), N-ethyl perfluorooctane sulfonamido acetic acid (N-EtFOSAA) and N-methyl perfluorooctane sulfonamido acetic acid (N-MeFOSAA) were also quantified.

The isomers of PFOA, PFOS and perfluorohexane sulfonate (PFHxS) were also analyzed. PFOA isomers contained linear PFOA (n-PFOA) and branched PFOA (br-PFOA) including iso-PFOA, 5m-PFOA, 4m-PFOA, 3m-PFOA and tb-PFOA; PFOS isomers contained linear PFOS (n-PFOS) and branched PFOS (br-PFOS) including iso-PFOS, (3+5) m-PFOS, 4m-PFOS, 1m-PFOS and m_2-PFOS; PFHxS isomers contained linear PFHxS (n-PFHxS) and branched PFHxS (br-PFHxS). The isomer nomenclature for PFOA, PFOS and PFHxS was determined following the system suggested by Benskin et al. (2007). For monomethyl branched isomers, perfluoroisopropyl isomers are abbreviated as iso- (e.g., perfluoroisopropyl-PFOA as iso-PFOA); m represents the perfluoromethyl branch, and the number before it indicates the carbon number on which the branch is situated (e.g., 4-perfluoromethyl-PFOA is named as 4m-PFOA). The tert-perfluorobutyl branched PFOA isomers are abbreviated as tb-PFOA, and the diperfluoromethyl branched PFOS isomers are abbreviated as m_2-PFOS. Together with above native standards (including PFAAs, isomers, alternatives and precursors), the corresponding mass-labeled PFAS were purchased from Wellington Laboratories

(Guelph, Ontario, Canada) for accurate quantification. More detailed information on the standards, reagents and nomenclature of different isomers can be found in the SI 1.2. Besides, the molecular structures and available physicochemical properties of individual PFAS are shown in Table S4 and S5. Based on carbon chain lengths, PFAAs are classified into short-chain (C4–C5), medium-chain (C6-C7) and long-chain (C8–C14) compounds, respectively (Wang et al., 2022b).

2.3 Sample pretreatment

Upon arrival at the laboratory, the collected samples underwent a thorough and systematic pretreatment process. Citrus tree organ samples were meticulously washed with distilled water followed by Milli-Q water. For branches, they were trimmed to approximately 5 cm lengths using pre-cleaned scissors, and then categorized based on their diameters (abbreviated as D) into three groups: less than 2 mm ($D \leq 2$ mm, thin), between 2 mm and 5 mm ($2 \text{ mm} < D \leq 5$ mm, middle) and greater than 5 mm ($D > 5$ mm, thick). The barks and woods of branches were carefully separated. Furthermore, the peels, pulps and seeds of citrus fruits were also divided. Subsequently, these distinct tissues were freeze-dried in a lyophilizer (-50℃ for 72h), then ground and homogenized in a knife mill. Soil samples were transferred to polypropylene (PP) boxes, air-dried, homogenized with a porcelain mortar and pestle, and sieved using a 2 mm mesh.

The pH was determined using a soil to 0.01 M $CaCl_2$ solution ratio of 1:5 (w/v) (Table S6), and soil organic matter (SOM) was measured utilizing the Walkley-Black procedure (Nelson and Sommers, 1983). Plant and soil samples were carefully extracted and purified primarily through solid phase extraction following methods previously

described by Felizeter et al. (2014) and Loi et al. (2011), respectively. Comprehensive information on sample pretreatment and extraction of citrus tree tissues and corresponding soils can be found in the SI 1.1 and 1.3.

2.4 Oxidation assay for precursors

The TOP assay was conducted to indirectly estimate the levels of unknown PFAA-precursors in a sample by oxidizing them into target PFCAs and measuring the incremental PFCAs (Δ[PFCAs]) (Houtz and Sedlak, 2012; Zhou et al., 2022). In brief, the extraction processes for citrus tree tissues and corresponding soils were consistent with the above extraction of target PFAS. The final methanolic extract of soil or plant samples in a 15 mL tube was evaporated using nitrogen gas before adding 12.0 mL of potassium persulfate ($K_2S_2O_8$) solution (20 g/L) and 0.23 mL of sodium hydroxide (NaOH) solution (10 M), followed by filling with ultrapure water to eliminate headspace. This resulted in concentrations of 60 mM for $K_2S_2O_8$ and 150 mM for NaOH. The samples were then heated at 85 ℃ for 20 h. After oxidation by heating, the samples were cooled in an ice water bath to room temperature, and solution's pH was neutralized with hydrochloric acid (HCl) to a range of 6.5–7.5 before further purification using solid phase extraction. Triplicates were performed for each sample. Detailed procedures of the TOP assay for plant and soil samples can be found in the SI 1.4.

2.5 Instrumental analysis

Quantitative analysis of target PFAS was conducted by high performance liquid chromatography coupled with electrospray ionization tandem mass spectrometry (Thermo Scientific UltiMate 3000 HPLC system and TSQ Altis triple-quadrupole mass

spectrometer, Thermo Fisher Scientific, USA) in the negative electrospray ionization (ESI) mode. In brief, the separation of 31 target PFAS was accomplished on an ZORBAX Eclipse Plus C18 column (2.1 mm × 100 mm, 3.5 μm, Agilent Technology, USA) with the injection volume of 5 μL, and a gradient elution program was applied using 2 mM ammonium acetate in Milli-Q water (phase A) and acetonitrile (phase B); the isomers of PFOS, PFOA and PFHxS were separated on a FluoroSep-RP Octyl column (150 × 2.1 mm, 3 μm, ES Industries, USA) with the injection volume of 10 μL, and 7 mM formic acid in Milli-Q water with pH adjusted to 4.0 using ammonium hydroxide (phase A) and methanol (phase B) were used as the mobile phase. The detailed descriptions and parameters of instrumental analysis are available in the SI 1.5 and Table S7, and the data processing was mainly based on TraceFinder (Thermo Fisher Scientific Co.).

2.6 Quality assurance/quality control (QA/QC)

Cross-contamination and PFAS-related experimental materials were minimized as much as possible throughout the study (detailly described in SI 1.6). To check for external contamination during sampling and extraction, field blanks, transport blanks and procedure blanks were conducted through regular analyses with each sample set. To examine carryover and background contamination during instrumental analysis, solvent blanks (LC-MS grade methanol) were run for each batch of 15 samples. The limit of quantification (LOQ) and limit of detection (LOD) were determined based on signal-to-noise (S/N) ratios of 10:1 and 3:1, respectively.

Quantification of the target PFAS was carried out using mass-labelled standard calibration curves containing 13 points ranging from 0.01 to 100 ng/mL and with regression coefficients greater than 0.99. To monitor the precision of extraction and analysis, replication experiments and instrumental drift assessments were performed for every sample set. The matrix spike recoveries (MSRs) and procedural spike recoveries (PSRs) of each target PFAS were evaluated by spiking a standard solution into different pollution-free matrices and anhydrous sodium sulfate, respectively. Detailed QA/QC information and quantification procedures can be found in SI 1.5 and 1.6 as well as in Table S8 and S9.

2.7 Data analysis

During the statistical analysis, concentrations less than the LOQ were assigned as one half of the LOQ, and those less than the LOD were given to values of $\mathrm{LOD}/\sqrt{2}$ (Hornung, 1990; Bao et al., 2011; Wang et al., 2014). To evaluate the contribution of specific fruit tissue (e.g., peel, pulp and seed) to the whole fruit bioaccumulation potential of target PFAS and unknown precursors (reflected by Δ[PFCAs]), a relative fruit burden (RFB) was according to Eq. (1) (Shi et al., 2018).

$$RFB_{tissue} = \frac{C_{tissue} \times f_{tissue}}{\sum_{n=1}^{i} C_{tissue,n} \times f_{tissue,n}} \times 100\% \quad (1)$$

Where C_{tissue} is the concentration of target PFAS or Δ[PFCAs] in a particular tissue (ng/g dry weight, dw) and the f_{tissue} represents the average mass fraction of specific fruit tissue (such as peel, pulp and seed) relative to the total fruit weight, which can be found in Table S10.

Bioaccumulation factor (BAF), which was expressed as the ratio of target PFAS concentration in citrus tree organ or tissue to that in corresponding soil on a dry weight basis, was calculated by Eq. (2) (Interstate Technology and Regulatory Council, 2020).

$$BAF = \frac{C_{organ\ or\ tissue}}{C_{soil}} \quad (2)$$

Where $C_{organ\ or\ tissue}$ is the concentration of target PFAS in a particular organ or tissue (ng/g dw) and C_{soil} means the concentration of target PFAS in corresponding soil (ng/g dw).

Based on averaging intake dose by body weight, the estimated daily intake (EDI, ng/kg·bw/day) of target PFAS or unknown precursors (reflected by Δ[PFCAs]) through citrus consumption can be calculated using Eq. (3) (Pan et al., 2021).

$$EDI = \frac{DC \times C_{citrus\ pulp}}{BW} \quad (3)$$

Where DC is the daily consumption of citrus pulp (g/d dw) for target group, $C_{citrus\ pulp}$ means the concentration of target PFAS or Δ[PFCAs] in citrus pulp (ng/g dw), and BW represents the body weight of target consumer (kg). Parameters used for calculation were according to survey data from the China Health and Nutrition Survey (CHNS) and the China Food Composition Tables (CFCT), illustrated in Table S11 (Chinese Center for Disease Control and University of North Carolina, 2019; Yang, 2018). The EDIs of PFAS via citrus consumption by different age groups of urban and rural residents were respectively estimated to assess potential health risks (SI 1.7 for details).

3 Results and discussion

3.1 Levels and profiles of PFAS in orchard soils

A total of 28 target PFAS were detected in orchard soils near the FCF. Higher levels of total target PFAS ($\sum PFAS_{target}$) in soils were found in Orchard 1 (73.1 ng/g dw) compared to Orchard 2 (31.5 ng/g dw), but the PFAS composition in both orchards was similar (Fig. 2A and Table S12). C6-C7 PFCAs, C8-C10 PFSAs and novel alternatives of PFCAs (such as GenX and HFPO-TA) were the primary target PFAS present in orchard soils, with average contributions of 35.9%, 23.0% and 14.9% respectively to $\sum PFAS_{target}$ (Fig. 2B). In addition to linear PFAS, branched isomers of PFOA (br-PFOA), PFOS (br-PFOS), and PFHxS (br-PFHxS) were also found in orchard soils, and both linear and branched isomers decreased as the distance from the FCF increased. In orchard soils, the average levels of br-PFOA were 1.32 g/g dw, accounting for about 35.1% of the ∑PFOA. Iso-PFOA, 5m-PFOA, tb-PFOA and 4m-PFOA were the major components of br-PFOA. The average concentrations of br-PFOS in soil samples were 3.01 ng/g dw, making up approximately 18.9% of the ∑PFOS; the main components of br-PFOS were iso-PFOS and (3+5)m-PFOS. Moreover, br-PFHxS were also detected in both orchard soils, accounting for about 19.5% of the ∑PFHxS (Table S13).

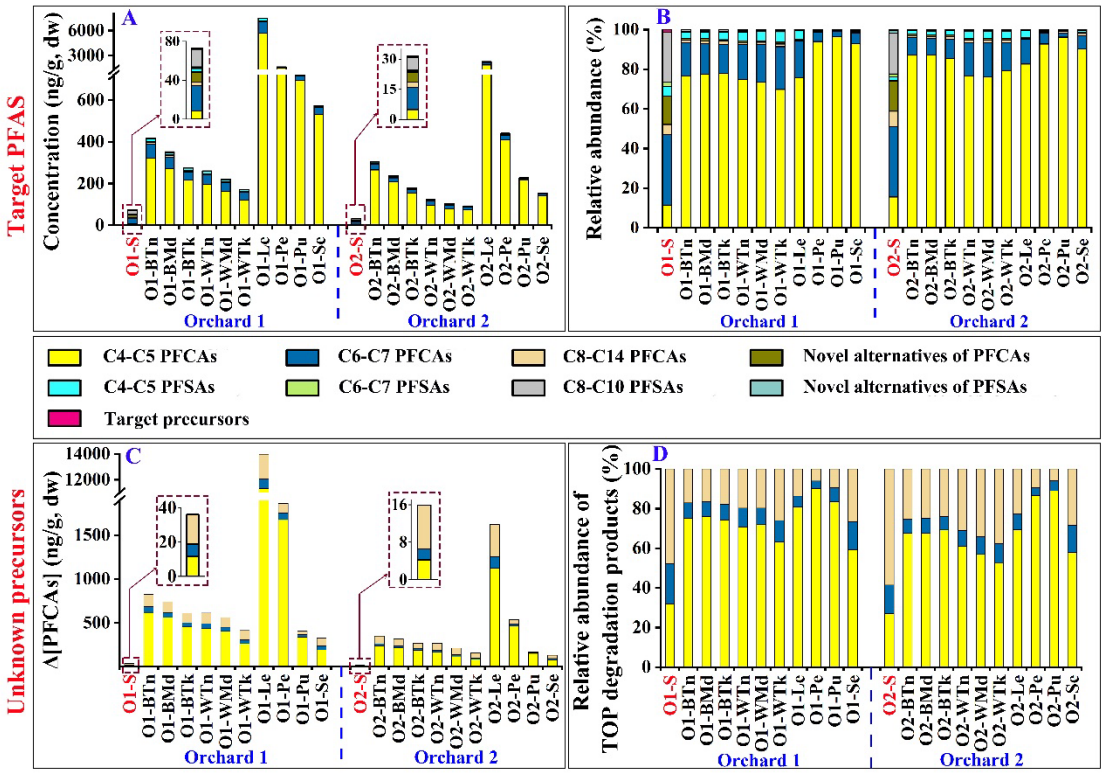

Fig.2. Concentrations and compositions of target PFAS and unknown precursors in orchard soils and citrus tree tissues.

Note: the abbreviations are explained as follows. O1: Orchard 1; O2: Orchard 2; S: soils, marked in red; BTn: barks of thin branches (D ≤ 2 mm); BMd: barks of middle branches (2 mm < D ≤ 5 mm); BTk: barks of thick branches (D > 5 mm); WTn: woods of thin branches (D ≤ 2 mm); WMd: woods of middle branches (2 mm < D ≤ 5 mm); WTk: woods of thick branches (D > 5 mm); D: the branch diameters; Le: leaves; Pe: peels; Pu: pulps; Se: seeds.

Despite the low levels of target precursors (FBSA, FHxSA, FOSA, N-MeFOSAA and N-EtFOSAA) detected in orchard soils (total, 0.21–0.92 ng/g dw), a large number of unknown precursors were found based on incremental PFCAs (named as Δ[PFCAs], degradation products of PFAA-precursors) after the TOP assay (Fig. 2C and Table S14). The measured ∑Δ[PFCAs] concentrations in soils were 36.2 ng/g dw in Orchard 1 and 15.9 ng/g dw in Orchard 2, respectively. C8-C14 PFCAs were the

dominant oxidation products of precursor compounds in orchard soils with an average incremental level of 13.3 ng/g dw, accounting for 53.2% of ∑Δ[PFCAs] (Fig. 2D).

3.2 Occurrence and tissue-specific distribution of PFAS in citrus trees

3.2.1 Concentrations and compositions of PFAS in citrus tree tissues

For PFAS detected in citrus tree tissues, the concentrations of $\sum PFAS_{target}$ in Orchard 1 and Orchard 2 were 1172–7496 ng/g dw and 92.5–2275 ng/g dw, respectively. Short-chain C4-C5 PFCAs (70.0–5343 ng/g dw) dominated in citrus tree tissues with an average relative abundance of 83.3% of the $\sum PFAS_{target}$ (Fig. 2A, 2B and Table S12), implying a bioaccumulation preference for these short-chain PFAS. Regarding isomer composition, the average proportions of br-PFOA, br-PFOS and br-PFHxS in citrus tree tissues were up to 37.2% of the ∑PFOA, 23.8% of the ∑PFOS and 32.3% of the ∑PFHxS, respectively. The high concentrations of unknown precursors (Orchard 1, 326–13979 ng/g dw; Orchard 2, 131–1623 ng/g dw) were also found in citrus tree tissues (Fig. 2C, Table S15). C4-C5 PFCAs became the predominant degradation products in citrus tree tissues, with an average incremental concentration of 953 ng/g dw, making up about 78.2% of the ∑Δ[PFCAs] (Fig. 2D). The ratios between incremental ∑PFCAs after the TOP assay to those before oxidation ($\sum\Delta[PFCA]/\sum[PFCA]_{before\ oxidation}$) in citrus tree tissues ranged from 0.57 to 2.72 with an average value of 1.63 (Table S15), indicating unknown precursors degradation may be an important source of target PFAS (McDonough et al., 2022; Zhou et al., 2021).

3.2.2 Distribution pattern of PFAS in leaves, branches and fruits

353 The concentrations of $\sum PFAS_{target}$ generally followed the order of leaves >
354 fruits > branches, which mainly reflected in the dominant component PFBA (Fig. 3A).
355 For PFBA, the average level was up to 3579 ng/g dw in leaves, followed by 611 ng/g
356 dw in fruits and 135 ng/g dw in branches. Extremely high concentrations in leaves may
357 be because that large amounts of PFBA were transported along with transpiration steam
358 in citrus trees and then accumulated in leaves, the major transpiration organs (Blaine et
359 al., 2013; Wang et al., 2020b). Waxy cuticles and stomata in leaves may also trap target
360 PFAS and unknown precursors in air and deposition, which were supported by the
361 evidence from high levels of total target PFAS (330 ng/L) and total unknown precursors
362 (2392 ng/L) in local precipitation (Liu et al., 2023). The precursors of short-chain PFAS
363 exhibited a higher biotransformation potential (Jiao et al., 2020), contributing to the
364 elevated levels of PFBA in leaves.

365 Compared with branches, fruits showed relatively higher concentrations of
366 PFBA. Fruits are the nutrient reservoir in citrus trees and PFBA could be transferred to
367 fruits along with nutrient delivery, but branches mainly acted as transient PFBA
368 transport channels along with nutrients and water (Huang et al., 2018; Paśko et al.,
369 2021). Thanks to the smaller molecule and higher hydrophilicity, PFBA exhibited a
370 higher translocation potential to leaves and fruits via branches (Felizeter et al., 2012;
371 Jiao et al., 2020). For medium- or long-chain PFCAs or more hydrophobic PFSAs, such
372 as PFHxA, PFOA, PFBS and PFHxS, the concentrations declined in the order: leaves >
373 branches > fruits (Fig. 3A), which might be due to the retention of these chemicals by
374 branch tissues (Blaine et al., 2014; Felizeter et al., 2014).

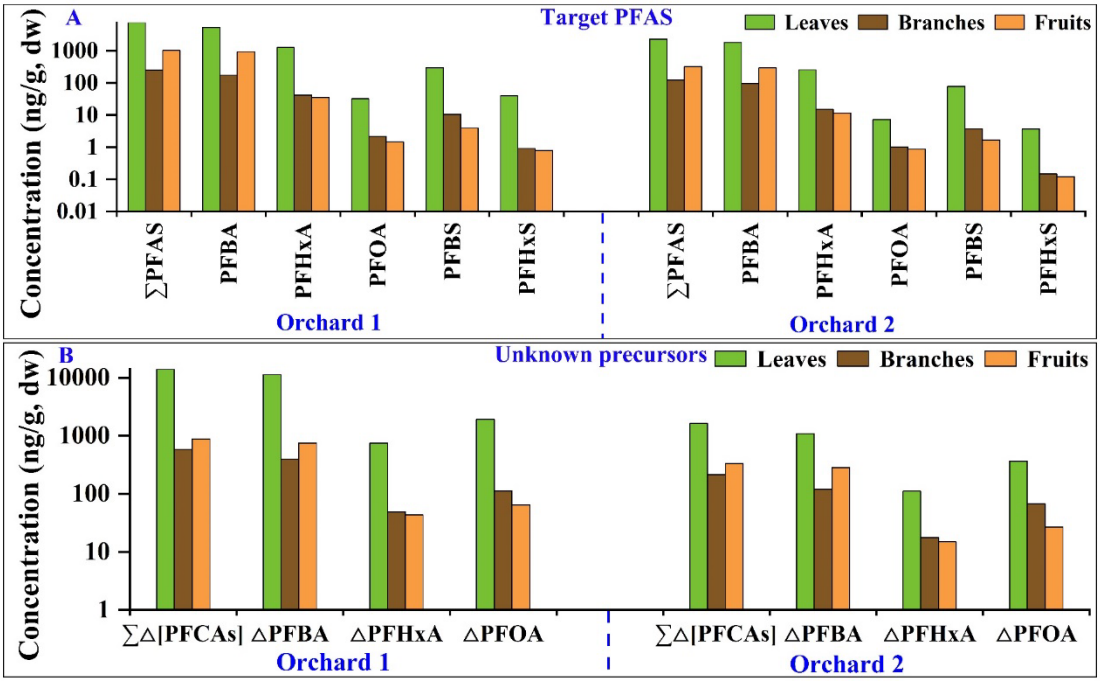

375

376 Fig.3. Tissue distribution of target PFAS and unknown precursors in leaves, branches and fruits

377 Unknown precursors exhibited higher levels in citrus trees than target PFAS,
378 and PFBA (C4), PFHxA (C6) and PFOA (C8) were dominant degradation products
379 (Fig. 3A and 3B). This observation may be associated with the potential air emission
380 of semi-volatile precursor products, including perfluorobutane sulfonyl fluoride
381 (PBSF), perfluorohexane sulfonyl fluoride (PHxSF), perfluorooctane sulfonyl fluoride
382 (POSF), and perfluorotributylamine (PFTBA), from the FCF during production (seeing
383 major products in SI 1.1). Leaves displayed much higher levels of different precursors
384 than branches and fruits, which can be mainly attributed to the capture of airborne
385 precursors by large areas of waxy cuticles and numerous stomata in leaves (Chen et al.,
386 2018; Tian et al., 2018). Compared with fruits, branches exhibited higher levels for the
387 precursors of PFHxA (ΔPFHxA) and PFOA (ΔPFOA), but lower levels for the
388 precursors of PFBA (ΔPFBA) (Fig. 3B). This finding may be because the more mobile
389 precursors of PFBA tend to accumulate in water-rich fruits, while those of PFHxA and

390 PFOA, being larger molecules, are more susceptible to being retained in branches
391 during transport.

392 **3.2.3 Distribution pattern of PFAS in branch woods and barks**

393 The concentrations of target PFAS in barks were greater than those in the
394 corresponding woods (Fig. 4A), which may result from different transport mechanisms
395 of PFAS in barks and woods. The transport of PFAS in wood primarily depends on less
396 obstructive vessels, whereas that mainly relies on more retentive sieve tubes in barks
397 (Cao et al., 2020; Comtet et al., 2017). Meanwhile, high protein contents in barks also
398 facilitate the affinity to PFAS (Azizpor et al., 2022).

399 Interestingly, the levels of individual target PFAS in barks and woods gradually
400 rose as the branch diameter decreased (Fig. 4A). This observation may be due to large
401 quantities of PFAS accumulated in leaves being translocated to other organs mainly via
402 bark sieve tubes from thin branches to thick ones. The transferred PFAS could be
403 preferentially retained by the barks of smaller diameter branches (Comtet et al., 2017).
404 Driven by transpiration steam, massive PFAS in wood vessels with fewer biological
405 barriers tend to transport from thick front branches to thin terminal ones (Lan et al.,
406 2018; Yu et al., 2021), likely resulting in higher concentrations of PFAS in woods of
407 smaller diameter branches. In addition, the higher accumulation potentials in the woods
408 of thin branches may also be partly contributed by the contamination transfer from
409 contacted barks with high levels of PFAS (Lu, 2003). Furthermore, higher levels of
410 unknown precursors of different chain-length PFAS (such as PFBA, PFHxA, and
411 PFOA) were also found in barks compared to woods, and those in both barks and woods

increased with diminishing branch diameters (Fig. 4B). Potential uptake of target PFAS and unknown precursors from air and deposition by exposed barks also contribute to higher contamination levels than those in corresponding woods (Jin et al., 2018; Liu et al., 2019).

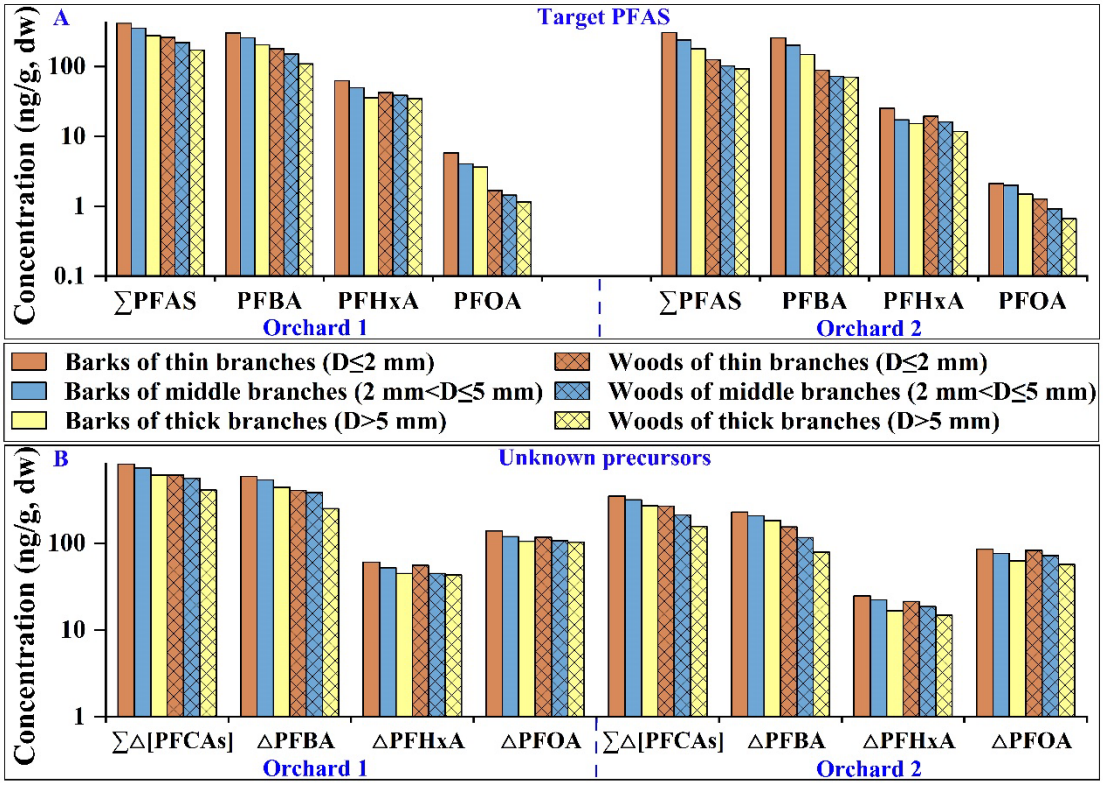

Fig.4. Tissue distribution of target PFAS and unknown precursors in branch woods and barks

Note: "D" represents the branch diameters.

3.2.4 Distribution pattern of PFAS in citrus peels, pulps and seeds

As the major target PFAS component in citrus fruits, PFBA exhibited the highest concentrations in peels, followed by pulps and then seeds, which was consistent with the concentrations of $\sum PFAS_{target}$. However, regarding the concentrations of medium- or long-chain PFCAs (e.g., PFHxA and PFOA) or more hydrophobic PFSAs (e.g., PFBS and PFHxS), the sequence displayed as peels > seeds > pulps (Fig. 5A). PFAS can be transported to fruits along with nutrients and water through branches.

Citrus peel is the tissue that connects the branch to the edible pulp, which may result in PFAS first entering the peel and then successively moving to the pulp and seed. As the first tissue in fruit being exposed to PFAS, peels also contain rich proteins (9.73%), facilitating the retention and bioaccumulation of PFAS (Romelle et al., 2016; Zhou et al., 2020). Due to the high-water content of pulps (87.8%) compared to seeds (5.3%) (Aranha and JoRGe, 2013; Chavan et al., 2018), pulps tended to accumulate PFBA that is more hydrophilic than its long-chain homologs. As the reproductive organs, citrus seeds contain much more proteins than pulps (seed, 12.8%; pulp, 1.2%) (Aranha and JoRGe, 2013; Yang, 2018), making seeds more prone to amass hydrophobic PFAS with medium or long carbon chains (e.g., PFHxA and PFOA) or sulfonate groups (e.g., PFBS and PFHxS).

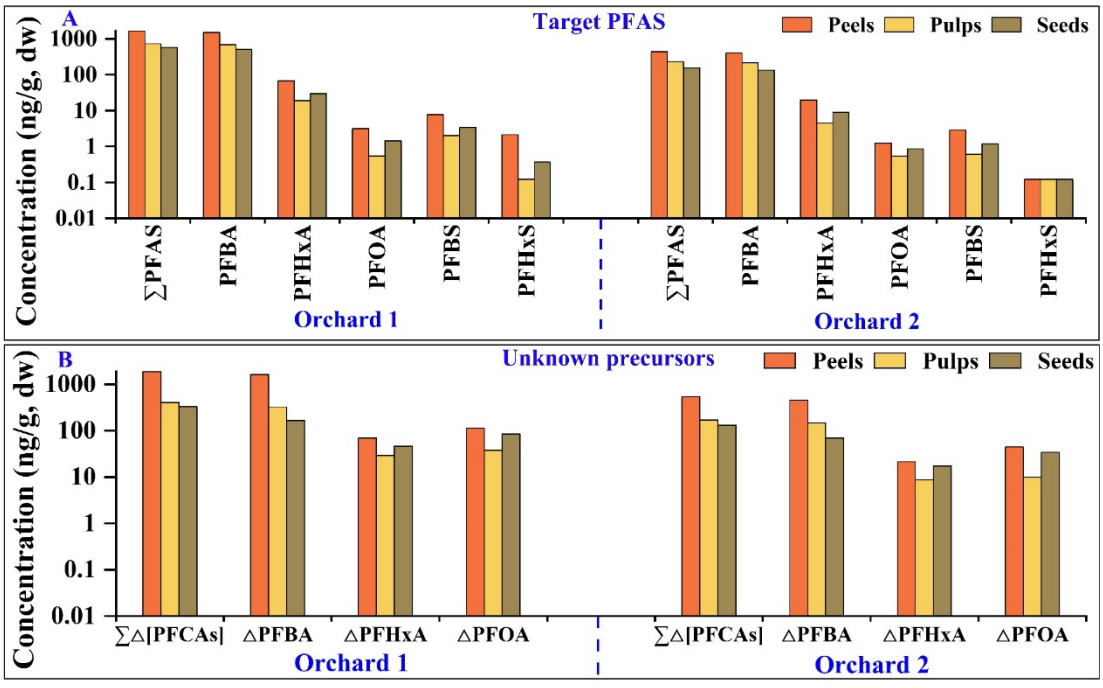

Fig.5. Tissue distribution of target PFAS and unknown precursors in citrus peels, pulps and seeds

It is worth noting that the concentrations of $\sum PFAS_{target}$ in citrus pulps on a wet weight (ww) basis (Orchard 1: 94.5 ng/g ww; Orchard 2: 29.8 ng/g ww) in this study

were much higher than those in fruits purchased from markets, such as apple (1.21 ng/g ww), pear (1.10 ng/g ww), strawberry (0.80 ng/g ww), lemon (0.78 ng/g ww), orange (0.72 ng/g ww), cherry (0.62 ng/g ww), grapefruit (0.09 ng/g ww), peach (0.09 ng/g ww), and grape (0.09 ng/g ww) (D'Hollander et al., 2015; Sznajder-Katarzynska et al., 2018). Therefore, potential health risks posed by consuming contaminated citruses in the study could need attention. Furthermore, large amounts of unknown precursors (131–1865 ng/g dw) in fruit tissues were also found based on the TOP assay. The concentrations of the precursors of PFBA (ΔPFBA: 69.1–1622 ng/g dw) in fruit tissues were peels > pulps > seeds. In contrast, for the precursors of PFHxA (ΔPFHxA: 8.70–68.7 ng/g dw) and PFOA (ΔPFOA: 9.84–112 ng/g dw), the corresponding levels were peels > seeds > pulps (Fig. 5B). This finding may be due to the precursors of more hydrophilic PFBA tending to accumulate in water-rich pulps, while those of more hydrophobic PFHxA and PFOA are susceptible to being amassed in seeds containing more proteins. Additionally, high levels of target PFAS and unknown precursors in citrus peels may be partly attributed to direct uptake from air and deposition (Liu et al., 2023; Wang et al., 2022a).

Upon evaluating the RFBs, it is clear that peels have a more significant impact on the overall fruit bioaccumulation potential of PFAS than the combined effects of pulps and seeds, even though pulps constitute the majority of the whole fruit weight (Table S10). For $\sum PFAS_{target}$, peels, pulps, and seeds contributed approximately 53.2%, 43.9%, and 2.9% to the total contamination burden of whole citrus fruits in Orchard 1; in Orchard 2, their respective contributions were 62.2%, 35.1%, and 2.7% (Fig. 6A).

For individual PFAS, pulps played a relatively more crucial role in the bioaccumulation of shorter-chain PFAS, and the relative burdens of pulps decreased with increasing carbon chain lengths of PFAS. This observation was supported by the evidence from relative burdens of pulps to PFBA (Orchard 1, 44.9%; Orchard 2, 36.4%), PFHxA (Orchard 1, 32.6%; Orchard 2, 19.1%), and PFHpA (Orchard 1, 12.7%; Orchard 2, 9.3%) (Fig. 6B, 6C and 6D). Regarding PFAS with the same carbon chain length, higher pulp burdens of PFBA with a carboxylic group (Orchard 1, 44.9%; Orchard 2, 36.4%) were observed compared to those of PFBS with a sulfonate group (Orchard 1, 31.5%; Orchard 2, 18.1%) (Fig. 6B and 6E).

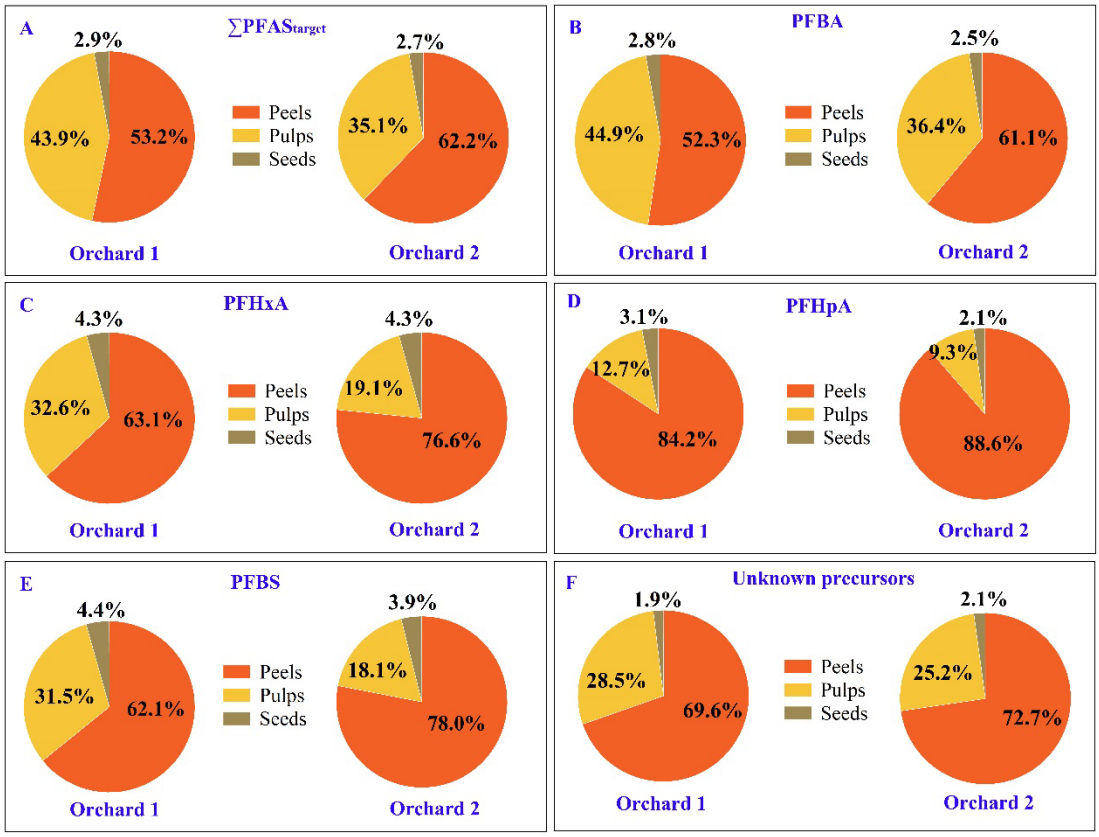

Fig.6. Relative burdens of different tissues to target PFAS and unknown precursors in fruits

Compared with pulps, peels displayed a higher relative burden for PFAS with longer carbon chain or sulfonate group (Fig. 6B, 6C, 6D, and 6E), primarily due to the

476 higher protein content in peels than in pulps (peels, 9.73%; pulps, 1.2%). Based on the
477 TOP assay, burden patterns of unknown precursors (reflected in Δ[PFCAs]) in different
478 fruit tissues were similar to those of $\sum PFAS_{target}$, but with a notable distinction of higher
479 relative burdens of $\sum\Delta$[PFCAs] in peels (Fig. 6F), which could be associated with the
480 large amounts of precursors in air and deposition (Liu et al., 2023; Tian et al., 2018).

481 **3.3 Bioaccumulation specificities of individual PFAS**

482 In general, citrus trees tended to accumulate shorter-chain PFAAs, and a linear
483 decrease in the logarithm of BAFs ($\log_{10}$BAFs) with increasing carbon chain lengths of
484 C4–C8 PFCAs and PFSAs was observed in various tissues, including leaves, branches
485 (barks and woods), and fruits (peels, pulps, and seeds) (Fig. 7A). Furthermore,
486 bioaccumulation potentials in citrus tree tissues varied for PFAAs with different
487 functional groups (Ghisi et al., 2019; Jiao et al., 2020). For PFAAs with the same carbon
488 chain length, PFCAs with a carboxylic group generally exhibited higher BAFs than
489 PFSAs with a sulfonate group (Fig. 7A). These findings may be attributed to the lower
490 K_{ow} values of PFAAs with shorter carbon chains or carboxylic groups, which display
491 stronger hydrophilicity and are more easily taken up by roots and transported to
492 different tissues of citrus trees (Blaine et al., 2013; Felizeter et al., 2014). It was
493 discovered that the $\log_{10}$BAF of individual linear PFAAs was linearly negatively
494 correlated with the corresponding logarithm of K_{ow} ($\log_{10} K_{ow}$) (Fig. S1).

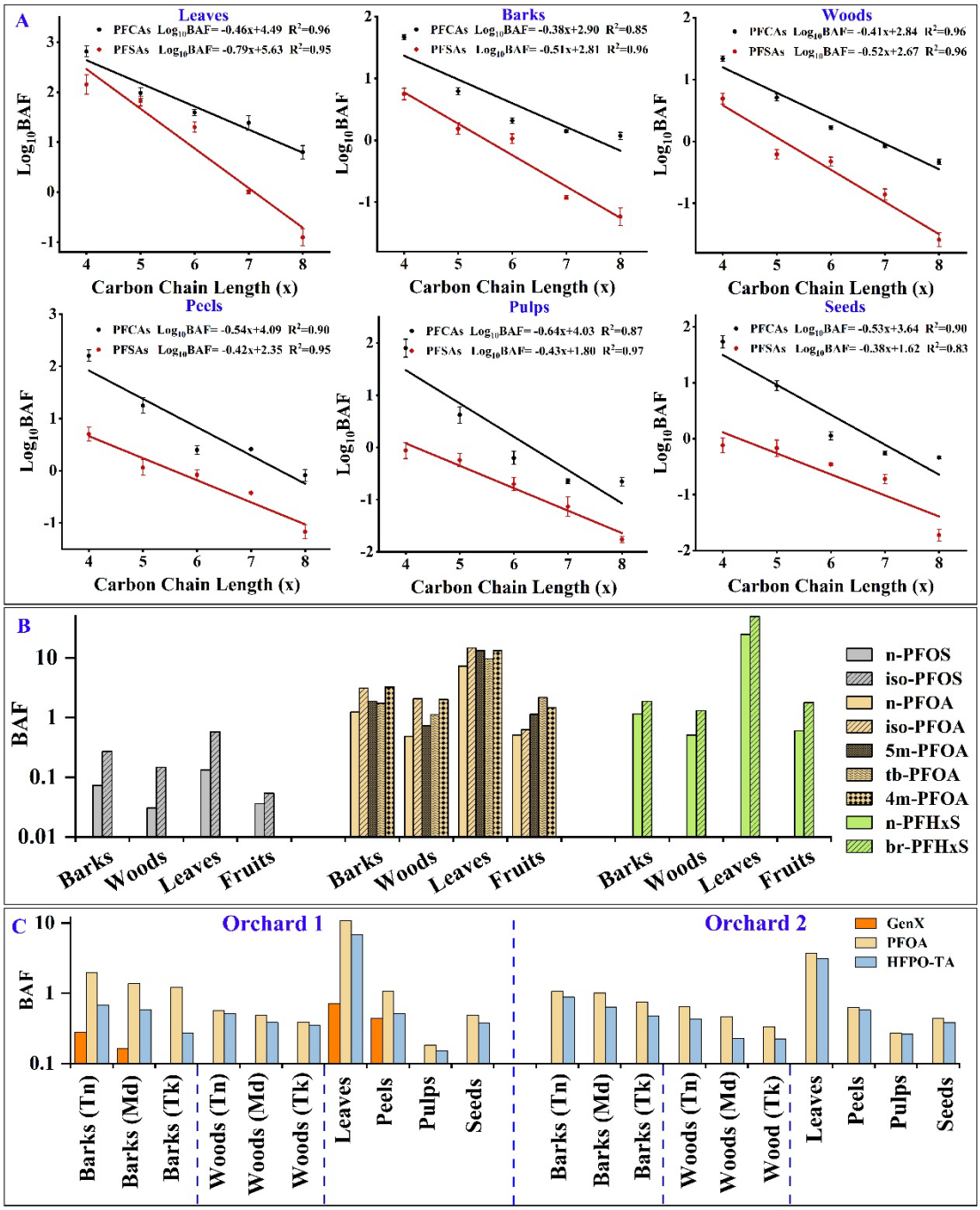

Fig. 7. Bioaccumulation factors (BAFs) of PFAS with different molecular structures in citrus tree tissues.

Note: the abbreviations are explained as follows. Tn: thin branches (D ≤ 2 mm); Md: middle branches (2 mm < D ≤ 5 mm); Tk: thick branches (D > 5 mm); D: the branch diameters.

Notably, compared to linear counterparts, higher BAFs of branched-chain isomers of PFOS, PFOA, and PFHxS demonstrated the isomer-specific

502 bioaccumulation capacities in citrus tree tissues (Fig. 7B). The greater hydrophilicity
503 of branched-chain isomers facilitates their root uptake from soils and more effective
504 transfer to citrus tree tissues (Chen et al., 2015; Schulz et al., 2020). PFEAs, such as
505 HFPO-TA and GenX, as novel alternatives to PFOA, exhibited lower bioaccumulation
506 capacities in various tissues of citrus trees compared with PFOA (Fig. 7C). This
507 phenomenon may be ascribed to the unique ether bond in carbon chains of these novel
508 chemicals, which could improve the sorption with soil minerals and result in reduced
509 mobility and bioavailability (Qi et al., 2022; Zhi et al., 2022). However, it was
510 suggested that the BAFs of PFOA were generally lower than those of GenX in rice
511 grains in a previous study (Liu et al., 2022). Such an opposite phenomenon may be
512 because that rice is cultivated in a water-soaked environment by most, and the more
513 soluble GenX appears to be more biologically effective under flooded conditions
514 (Wang et al., 2019; Yamazaki et al., 2023).

515 Compared to those in leaves of local vegetables (e.g., carrot, 67.1; asparagus
516 lettuce, 19.9; Chinese cabbage, 61.3) (Liu et al., 2023), much higher BAFs of
517 $\sum PFAS_{target}$ (up to 104) were found in citrus tree leaves in this study, possibly resulting
518 from their longer growth period. However, compared to different edible parts of
519 vegetables grown in this area (such as edible roots, stems, and leaves), citrus pulps
520 exhibited lower bioaccumulation potentials of PFAS of varying carbon chain lengths
521 and functional groups, which was supported by the evidence from the BAFs of PFBA,
522 PFHxA, PFOA, PFBS, PFHxS and GenX in citrus pulps, radish roots, asparagus lettuce
523 stems, and Chinese cabbage leaves (Fig. S2). This finding may be ascribed to greater

retention due to longer distances and more biological barriers during PFAS transport to fruit pulps. Therefore, compared to vegetables, citrus tree planting could be an effective strategy to reduce crop bioaccumulation and potential environmental risks of PFAS in contaminated agricultural lands.

3.4 Human exposure estimation and health risks of PFAS for local urban and rural residents via contaminated citrus fruits

Since significant amounts of unknown precursors may be transformed into target PFAS during digestion and other biochemical processes in the human body (Berhanu et al., 2023; Wen et al., 2018), the human exposure risks may be underestimated based on the detected target PFAS alone (Diao et al., 2022; McDonough et al., 2022). In order to evaluate the underestimation of PFAS through citrus consumption for local residents, the comparison was conducted for human exposure risks between ignoring and considering degradation potentials. Human exposure estimation was based on the total and individual PFAS concentrations in citrus at upper limits and dietary habits of local urban and rural residents. If we only considered detected target PFAS and neglected degradation potentials of precursors in citrus pulps, as is traditionally done in human exposure and risk assessment, the EDIs of PFOA, PFHxA, and PFBA would be underestimated by factors of about 70, 1.6, and 0.5, respectively (Fig. 8A and 8B, Table S16). Based on the TOP assay, the overall contribution of potential precursor degradation to human exposure to PFAS via citrus consumption was estimated to be approximately 36%, with individual exposure contributions of 32.5% to PFBA, 61.1% to PFHxA, and 98.6% to PFOA (Fig. 8C).

These new findings demonstrate that taking into account precursor degradation potentials in human exposure and risk assessment is critical for better protection of fruit consumers.

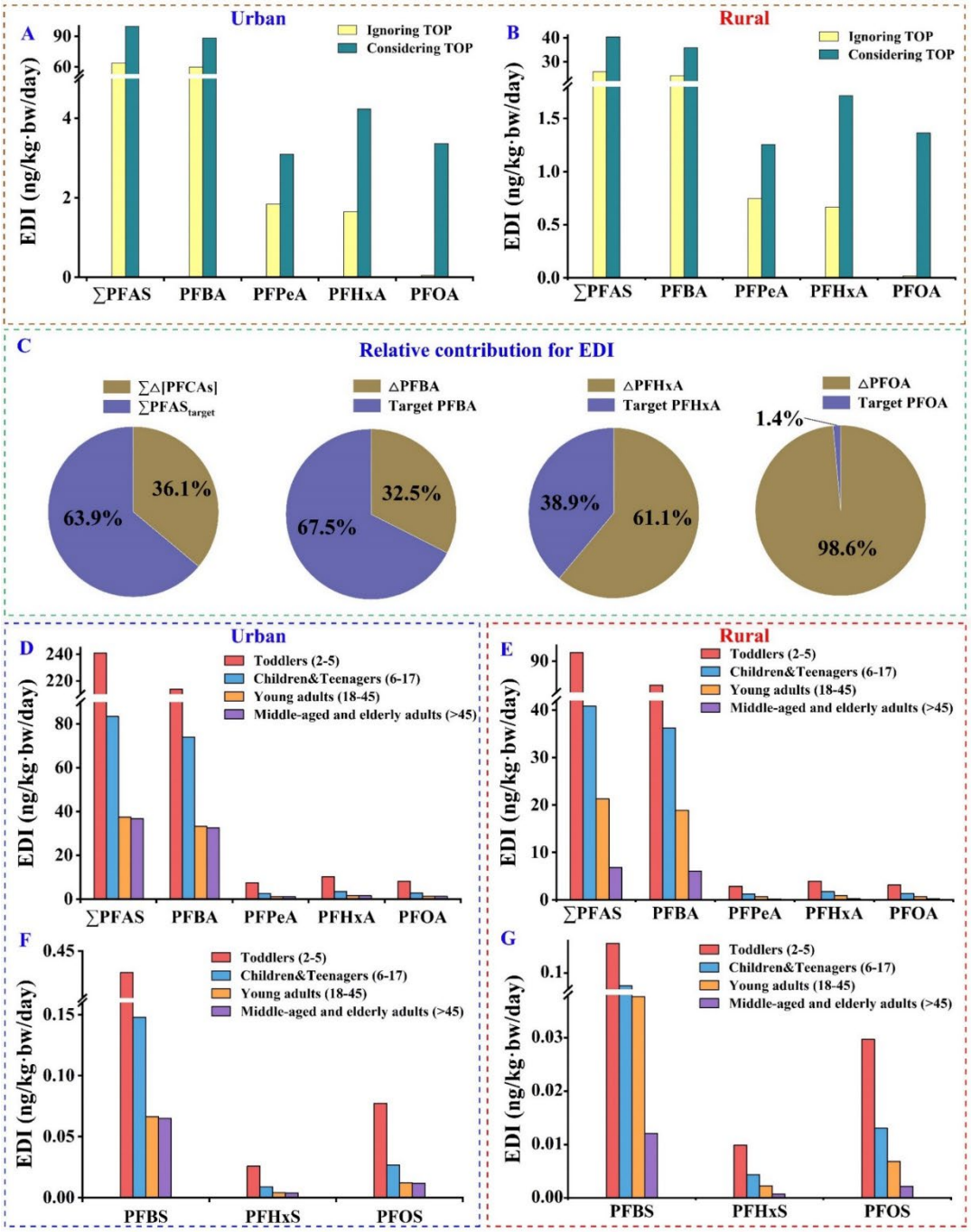

Fig. 8. Estimated daily intakes (EDIs) of PFAS via the consumption of contaminated citruses (ng/kg·bw/day) for local urban and rural residents with considering or ignoring TOP.

As such, the TOP assay was taken into account along with detected target PFAS in citrus pulps, aiming to provide a more comprehensive health risk assessment. In general, the EDIs of ∑PFAS were highest for toddlers (241 ng/kg·bw/day in urban; 92.7 ng/kg·bw/day in rural) mainly owing to their higher consumption per body weight, and showed a declining trend with increasing age groups (Fig. 8D and 8E). Much higher EDIs of PFAS for different age groups in urban rather than rural areas were likely due to citrus consumption preferences in local urban diets (Fig. 8D, 8E, 8F and 8G). Notably, the EDIs of PFAS through consuming contaminated citruses highlight the necessity for human health risk assessment. Although there is a lack of guidelines for dietary intake of PFAS in China, tolerable daily intake (TDI) values for some PFAS have been set in other parts of the world. For legacy long-chain PFAAs, PFOA (0.23–8.14 ng/kg·bw/day) showed much higher EDIs than PFOS (0.002–0.08 ng/kg·bw/day), with the maximum EDI of PFOA (8.14 ng/kg·bw/day) being higher than its TDI value (3 ng/kg·bw/day) proposed by U.S. Agency for Toxic Substances & Disease Registry (ATSDR) and close to the magnitude order of its TDI value (20 ng/kg·bw/day) recommended by U.S. Environmental Protection Agency (USEPA) (ATSDR, 2018; USEPA, 2016), suggesting potential health risks. According to the Minnesota Department of Health, the TDI values for PFBA, PFHxA, and PFBS were evaluated as 2900, 150, and 84 ng/kg·bw/day, respectively (Minnesota Department of Health, 2018, 2021, 2022). Despite that the EDIs of PFBA (6.05–214 ng/kg·bw/day), PFHxA (0.29–10.2 ng/kg·bw/day), and PFBS (0.01–0.43 ng/kg·bw/day) via consumption of contaminated citruses were much lower than their corresponding TDI values (Table

574 S17), the human exposure of these short-chain PFAS may exacerbate cumulative health
575 risks, mainly due to their similar toxic effects to PFOA and higher placental transfer
576 efficiency (Gao et al., 2019).

577 **4. Conclusions and perspectives**

578 The results of this study indicate that planting citrus in contaminated fields nearby
579 the FCF may result in concerning levels of target PFAS and unknown precursors in
580 multiple citrus tree tissues. Short-chain, branched or carboxylic acid-based PFAS
581 generally showed higher bioaccumulation capacities than their relatively hydrophobic
582 counterparts in citrus tree tissues; while alternative PFEAs (e.g., HFPO-TA and GenX)
583 exhibited lower BAFs than structurally similar PFAAs. On the whole, more hydrophilic
584 PFAS and precursors demonstrated higher translocation potentials and tended to
585 accumulate in water-rich tissues (for example citrus pulps); while more hydrophobic
586 ones were susceptible to be retained by biological barriers and amassed in protein-rich
587 tissues (such as barks, peels and seeds). Among all citrus tree tissues, the highest
588 concentrations of target PFAS and unknown precursors were found in leaves.

589 Given that the much lower bioaccumulation potentials of PFAS in citrus pulps
590 compared with edible parts of different vegetables, planting citrus trees may be an
591 alternative strategy to reduce the pollution of plant-derived foods from contaminated
592 fields, but it should be a concern of potential environmental hazards posed by heavily-
593 contaminated fallen leaves and peels. When assessing the human health risk from
594 contaminated citrus, precursor degradation, often not being taken into account, was
595 found to contribute considerably to total PFAS exposure, and this finding facilitated to

advance a more comprehensive risk assessment of PFAS from citrus ingestion or other exposure pathways to safeguard public health. Moreover, more toxicological studies on the cumulative hazards of PFAAs, alternatives and precursors are urgently needed to precisely evaluate their health threats.

CRediT author statement

Shun Liu: Investigation, Resources, Formal analysis, Data curation, Writing - Original Draft, Visualization. **Zhaoyang Liu:** Conceptualization, Methodology, Validation, Writing - Review & Editing, Supervision, Project administration, Funding acquisition. **Feng Xiao:** Conceptualization, Writing - Review & Editing. **Mingxia Wang:** Writing - Review & Editing. **Chang Chen:** Writing - Review & Editing. **Xiang Wan:** Writing - Review & Editing. **Hao Guo:** Investigation. **Ziyao Luo:** Investigation. **Linlin Zhong:** Resources. **Jay Gan:** Writing - Review & Editing. **Wenfeng Tan:** Supervision, Writing - Review & Editing, Funding acquisition.

Declaration of Competing Interest

The authors declare that they have no known competing financial interests or personal relationships that could have appeared to influence the work reported in this paper.

Acknowledgments

This study was supported by the National Natural Science Foundation of China [grant number 41807137], Natural Science Foundation of Hubei Province [grant number 2022CFB284 and grant number 2020CFA013], Project 2662021ZHQD001 supported by the Fundamental Research Funds for the Central Universities, National Key Research and Development Program of China [grant number 2020YFC1807001]. We would like to thank the editors and reviewers for their valuable comments and suggestions.

References

Agency for Toxic Substances and Disease Registry. 2018. Toxicological Profile for Perfluoroalkyls (Draft for Public Comment). US Department of Health and Human Services, Public Health Service Atlanta, GA.

Aranha, C.P.M. and JoRGe, N. 2013. Physico-chemical characterization of seed oils extracted from oranges (Citrus sinensis). Food Science and Technology Research 19(3), 409-415.

Azizpor, P., Sullivan, L., Lim, A. and Groover, A. 2022. Facile labeling of sieve element phloem-protein bodies using the reciprocal oligosaccharide probe OGA (488). Frontiers in Plant Science 13, 809923.

Bao, J., Liu, W., Liu, L., Jin, Y., Dai, J., Ran, X., Zhang, Z. and Tsuda, S. 2011. Perfluorinated compounds in the environment and the blood of residents living near fluorochemical plants in Fuxin, China. Environmental Science & Technology 45(19), 8075-8080.

Barzen-Hanson, K.A., Roberts, S.C., Choyke, S., Oetjen, K., McAlees, A., Riddell, N., McCrindle, R., Ferguson, P.L., Higgins, C.P. and Field, J.A. 2017. Discovery of 40 classes of per-and polyfluoroalkyl substances in historical aqueous film-forming foams (AFFFs) and AFFF-impacted groundwater. Environmental Science & Technology 51(4), 2047-2057.

Benskin, J.P., Bataineh, M. and Martin, J.W. 2007. Simultaneous characterization of perfluoroalkyl carboxylate, sulfonate, and sulfonamide isomers by liquid chromatography-tandem mass spectrometry. Analytical Chemistry 79(17), 6455-6464.

Berhanu, A., Mutanda, I., Taolin, J., Qaria, M.A., Yang, B. and Zhu, D. 2023. A review of microbial degradation of per-and polyfluoroalkyl substances (PFAS): Biotransformation routes and enzymes. Science of The Total Environment 859, 160010.

Blaine, A.C., Rich, C.D., Hundal, L.S., Lau, C., Mills, M.A., Harris, K.M. and Higgins, C.P. 2013. Uptake of perfluoroalkyl acids into edible crops via land applied biosolids: field and greenhouse studies. Environmental Science & Technology 47(24), 14062-14069.

Blaine, A.C., Rich, C.D., Sedlacko, E.M., Hundal, L.S., Kumar, K., Lau, C., Mills, M.A., Harris, K.M. and Higgins, C.P. 2014. Perfluoroalkyl acid distribution in various plant compartments of edible crops grown in biosolids-amended soils. Environmental Science & Technology 48(14), 7858-7865.

Cao, Y., Ma, C., Chen, H., Zhang, J., White, J.C., Chen, G. and Xing, B. 2020. Xylem-based long-distance transport and phloem remobilization of copper in Salix integra Thunb. Journal of Hazardous Materials 392, 122428.

Chinese Center for Disease Control and University of North Carolina, 2019. China Health and Nutrition Survey. https://www.cpc.unc.edu/projects/china/data/datasets/index.html (accessed 29th May 2023).

Chang, C.J., Barr, D.B., Ryan, P.B., Panuwet, P., Smarr, M.M., Liu, K., Kannan, K., Yakimavets, V., Tan, Y., Ly, V., Marsit, C.J., Jones, D.P., Corwin, E.J., Dunlop, A.L. and Liang, D. 2022. Per- and polyfluoroalkyl substance (PFAS) exposure, maternal metabolomic perturbation, and fetal growth in African American women: A meet-in-the-middle approach. Environment International 158, 106964.

Chavan, P., Singh, A.K. and Kaur, G. 2018. Recent progress in the utilization of industrial waste and by-products of citrus fruits: A review. Journal of Food Process Engineering 41(8), e12895.

Chen, H., Yao, Y., Zhao, Z., Wang, Y., Wang, Q., Ren, C., Wang, B., Sun, H., Alder, A.C. and Kannan, K. 2018. Multimedia Distribution and Transfer of Per- and Polyfluoroalkyl Substances (PFASs) Surrounding Two Fluorochemical Manufacturing Facilities in Fuxin, China. Environ Sci Technol 52(15), 8263-8271.

Chen, X., Zhu, L., Pan, X., Fang, S., Zhang, Y. and Yang, L. 2015. Isomeric specific partitioning behaviors of perfluoroalkyl substances in water dissolved phase, suspended particulate matters and sediments in Liao River Basin and Taihu Lake, China. Water Research 80, 235-244.

Comtet, J., Jensen, K.H., Turgeon, R., Stroock, A.D. and Hosoi, A. 2017. Passive phloem loading and long-distance transport in a synthetic tree-on-a-chip. Nature Plants 3(4), 1-8.

Cui, Q., Pan, Y., Zhang, H., Sheng, N., Wang, J., Guo, Y. and Dai, J. 2018. Occurrence and tissue distribution of novel perfluoroether carboxylic and sulfonic acids and legacy per/polyfluoroalkyl substances in black-spotted frog (Pelophylax nigromaculatus). Environmental Science & Technology 52(3), 982-990.

D'Hollander, W., Herzke, D., Huber, S., Hajslova, J., Pulkrabova, J., Brambilla, G., De Filippis, S.P., Bervoets, L. and de Voogt, P. 2015. Occurrence of perfluorinated alkylated substances in cereals, salt, sweets and fruit items collected in four European countries. Chemosphere 129, 179-185.

Diao, J., Chen, Z., Wang, T., Su, C., Sun, Q., Guo, Y., Zheng, Z., Wang, L., Li, P. and Liu, W. 2022. Perfluoroalkyl substances in marine food webs from South China Sea: Trophic transfer and human exposure implication. Journal of Hazardous Materials 431, 128602.

Dick, R.P., Thomas, D.R. and Halvorson, J.J. 1997. Standardized methods, sampling, and sample pretreatment. Methods for assessing soil quality 49, 107-121.

Eun, H., Yamazaki, E., Taniyasu, S., Miecznikowska, A., Falandysz, J. and Yamashita, N. 2020. Evaluation of perfluoroalkyl substances in field-cultivated vegetables. Chemosphere 239, 124750.

Evich, M.G., Davis, M.J., McCord, J.P., Acrey, B., Awkerman, J.A., Knappe, D.R., Lindstrom, A.B., Speth, T.F., Tebes-Stevens, C. and Strynar, M.J. 2022. Per-and polyfluoroalkyl substances in the environment. Science 375(6580), eabg9065.

Felizeter, S., McLachlan, M.S. and de Voogt, P. 2012. Uptake of perfluorinated alkyl acids by hydroponically grown lettuce (Lactuca sativa). Environmental Science & Technology 46(21), 11735-11743.

Felizeter, S., McLachlan, M.S. and De Voogt, P. 2014. Root uptake and translocation of perfluorinated alkyl acids by three hydroponically grown crops. Journal of Agricultural and Food Chemistry 62(15), 3334-3342.

Gao, K., Zhuang, T., Liu, X., Fu, J., Zhang, J., Fu, J., Wang, L., Zhang, A., Liang, Y., Song, M. and Jiang, G. 2019. Prenatal exposure to per- and polyfluoroalkyl substances (PFASs) and association between the placental transfer efficiencies and dissociation constant of serum proteins-PFAS complexes. Environmental Science & Technology 53(11), 6529-6538.

Ghisi, R., Vamerali, T. and Manzetti, S. 2019. Accumulation of perfluorinated alkyl substances (PFAS) in agricultural plants: A review. Environmental Research 169, 326-341.

Gomis, M.I., Vestergren, R., Borg, D. and Cousins, I.T. 2018. Comparing the toxic potency in vivo of long-chain perfluoroalkyl acids and fluorinated alternatives. Environment International 113, 1-9.

Greenhill, C. 2017. PFASs, sex hormones and asthma. Nature Reviews Endocrinology 13(7), 377-377.

Hornung, R.W. and Reed, L.D. 1990. Estimation of average concentration in the presence of nondetectable values. Applied occupational and environmental hygiene 5(1), 46-51.

Houtz, E.F. and Sedlak, D.L. 2012. Oxidative conversion as a means of detecting precursors to perfluoroalkyl acids in urban runoff. Environmental Science & Technology 46(17), 9342-9349.

Huang, C.W., Domec, J.C., Palmroth, S., Pockman, W.T., Litvak, M.E. and Katul, G.G. 2018. Transport in a coordinated soil-root-xylem-phloem leaf system. Advances in water resources 119, 1-16.

Interstate Technology and Regulatory Council, 2020. PFAS Technical and Regulatory Guidance Document and Fact Sheets PFAS-1. Washington, DC. https://pfas-1.itrcweb.org/ (Accessed 29th May 2023).

Jiao, X., Shi, Q. and Gan, J. 2020. Uptake, accumulation and metabolism of PFASs in plants and health perspectives: a critical review. Critical Reviews in Environmental Science and Technology 51(23), 2745-2776.

718 Jin, B., Mallula, S., Golovko, S.A., Golovko, M.Y. and Xiao, F. 2020. In vivo generation of PFOA,
719 PFOS, and other compounds from cationic and zwitterionic per-and polyfluoroalkyl substances
720 in a terrestrial invertebrate (Lumbricus terrestris). Environmental Science & Technology 54(12),
721 7378-7387.
722 Jin, H., Shan, G., Zhu, L., Sun, H. and Luo, Y. 2018. Perfluoroalkyl acids including isomers in tree
723 barks from a Chinese fluorochemical manufacturing park: implication for airborne
724 transportation. Environmental Science & Technology 52(4), 2016-2024.
725 Klenow, S., Heinemeyer, G., Brambilla, G., Dellatte, E., Herzke, D. and de Voogt, P. 2013. Dietary
726 exposure to selected perfluoroalkyl acids (PFAAs) in four European regions. Food Additives &
727 Contaminants: Part A 30(12), 2141-2151.
728 Lan, Z., Zhou, M., Yao, Y. and Sun, H. 2018. Plant uptake and translocation of perfluoroalkyl acids in
729 a wheat-soil system. Environmental Science and Pollution Research 25(31), 30907-30916.
730 Li, P., Oyang, X., Zhao, Y., Tu, T., Tian, X., Li, L., Zhao, Y., Li, J. and Xiao, Z. 2019. Occurrence of
731 perfluorinated compounds in agricultural environment, vegetables, and fruits in regions
732 influenced by a fluorine-chemical industrial park in China. Chemosphere 225, 659-667.
733 Lim, X.Z., 2019. Tainted water: the scientists tracing thousands of fluorinated chemicals in our
734 environment. Nature 566(7742), 26-29.
735 Liu, S., Liu, Z., Tan, W., Johnson, A.C., Sweetman, A.J., Sun, X., Liu, Y., Chen, C., Guo, H. and Liu,
736 H. 2023. Transport and transformation of perfluoroalkyl acids, isomer profiles, novel
737 alternatives and unknown precursors from factories to dinner plates in China: New insights into
738 crop bioaccumulation prediction and risk assessment. Environment International, 107795.
739 Liu, Y., Hou, X., Chen, W., Kong, W., Wang, D., Liu, J. and Jiang, G. 2019. Occurrences of
740 perfluoroalkyl and polyfluoroalkyl substances in tree bark: Interspecies variability related to
741 chain length. Science of the Total Environment 689, 1388-1395.
742 Liu, Z., Lu, Y., Shi, Y., Wang, P., Jones, K., Sweetman, A.J., Johnson, A.C., Zhang, M., Zhou, Y., Lu,
743 X., Su, C., Sarvajayakesavaluc, S. and Khan, K. 2017. Crop bioaccumulation and human
744 exposure of perfluoroalkyl acids through multi-media transport from a mega fluorochemical
745 industrial park, China. Environment International 106, 37-47.
746 Liu, Z., Xu, C., Johnson, A.C., Sun, X., Ding, X., Ding, D., Liu, S. and Liang, X. 2022. Source
747 apportionment and crop bioaccumulation of perfluoroalkyl acids and novel alternatives in an
748 industrial-intensive region with fluorochemical production, China: Health implications for
749 human exposure. Journal of Hazardous Materials 423(Pt A), 127019.

Loi, E.I., Yeung, L.W., Taniyasu, S., Lam, P.K., Kannan, K. and Yamashita, N. 2011. Trophic magnification of poly- and perfluorinated compounds in a subtropical food web. Environmental Science & Technology 45(13), 5506-5513.

Lu, J., 2003. Plant Nutrition (in Chinese), Chinese Agricultural University Press: Beijing, China.

McDonough, C.A., Li, W., Bischel, H.N., De Silva, A.O. and DeWitt, J.C. 2022. Widening the lens on PFASs: direct human exposure to perfluoroalkyl acid precursors (pre-PFAAs). Environmental Science & Technology 56(10), 6004-6013.

Minnesota Department of Health, 2018. Toxicological Summary for: Perfluorobutanoate. https://www.health.state.mn.us/communities/environment/risk/docs/guidance/gw/pfba2summ.pdf. (Accessed 29th May 2023).

Minnesota Department of Health, 2021. Toxicological Summary for: Perfluorohexanoat. https://www.health.state.mn.us/communities/environment/risk/docs/guidance/gw/pfhxa.pdf. (Accessed 29th May 2023).

Minnesota Department of Health, 2022. Toxicological Summary for: Perfluorobutane sulfonate. https://www.health.state.mn.us/communities/environment/risk/docs/guidance/gw/pfbssummary.pdf. (Accessed 29th May 2023).

Munoz, G., Desrosiers, M., Vetter, L., Vo Duy, S., Jarjour, J., Liu, J. and Sauve, S. 2020. Bioaccumulation of zwitterionic polyfluoroalkyl substances in earthworms exposed to aqueous film-forming foam impacted soils. Environmental Science & Technology 54(3), 1687-1697.

Nelson, D.a. and Sommers, L.E. 1983. Total carbon, organic carbon, and organic matter. Methods of soil analysis: Part 2 chemical and microbiological properties 9, 539-579.

Pan, C.-G., Xiao, S.-K., Yu, K.-F., Wu, Q. and Wang, Y.-H. 2021. Legacy and alternative per-and polyfluoroalkyl substances in a subtropical marine food web from the Beibu Gulf, South China: Fate, trophic transfer and health risk assessment. Journal of Hazardous Materials 403, 123618.

Pan, Y., Zhang, H., Cui, Q., Sheng, N., Yeung, L.W.Y., Guo, Y., Sun, Y. and Dai, J. 2017. First report on the occurrence and bioaccumulation of hexafluoropropylene oxide trimer acid: an emerging concern. Environmental Science & Technology 51(17), 9553-9560.

Pan, Y., Zhang, H., Cui, Q., Sheng, N., Yeung, L.W.Y., Sun, Y., Guo, Y. and Dai, J. 2018. Worldwide distribution of novel perfluoroether carboxylic and sulfonic acids in surface water. Environmental Science & Technology 52(14), 7621-7629.

Pasecnaja, E., Bartkevics, V. and Zacs, D. 2022. Occurrence of selected per-and polyfluorinated alkyl substances (PFASs) in food available on the European market–A review on levels and human exposure assessment. Chemosphere 287, 132378.

783 Paśko, P., Galanty, A., Zagrodzki, P., Luksirikul, P., Barasch, D., Nemirovski, A. and Gorinstein, S.
784 2021. Dragon fruits as a reservoir of natural polyphenolics with chemopreventive properties.
785 Molecules 26(8), 2158.
786 Qi, Y., Cao, H., Pan, W., Wang, C. and Liang, Y. 2022. The role of dissolved organic matter during
787 Per-and Polyfluorinated Substance (PFAS) adsorption, degradation, and plant uptake: A review.
788 Journal of Hazardous Materials, 129139.
789 Qin, H., Niu, Y., Luan, H., Li, M., Zheng, L., Pan, Y. and Liu, W. 2022. Effects of legacy and emerging
790 per- and polyfluoroalkyl substances on PPARalpha/beta/gamma regulation and
791 osteogenic/adipogenic differentiation. Environment International 170, 107584.
792 Romelle, F.D., Rani, A. and Manohar, R.S. 2016. Chemical composition of some selected fruit peels.
793 European Journal of Food Science and Technology 4(4), 12-21.
794 Ryan, J.J., Pilon, J.-C. and Leduc, R. 1982. Composite sampling in the determination of pyrethrins in
795 fruit samples. Journal of the Association of Official Analytical Chemists 65(4), 904-908.
796 Schulz, K., Silva, M.R. and Klaper, R. 2020. Distribution and effects of branched versus linear isomers
797 of PFOA, PFOS, and PFHxS: A review of recent literature. Science of the Total Environment
798 733, 139186.
799 Shi, Y., Vestergren, R., Nost, T.H., Zhou, Z. and Cai, Y. 2018. Probing the differential tissue distribution
800 and bioaccumulation behavior of per-and polyfluoroalkyl substances of varying chain-lengths,
801 isomeric structures and functional groups in crucian carp. Environmental Science & Technology
802 52(8), 4592-4600.
803 Sznajder-Katarzynska, K., Surma, M., Cieslik, E. and Wiczkowski, W. 2018. The perfluoroalkyl
804 substances (PFASs) contamination of fruits and vegetables. Food Additives & Contaminants:
805 Part A 35(9), 1776-1786.
806 Tian, Y., Yao, Y., Chang, S., Zhao, Z., Zhao, Y., Yuan, X., Wu, F. and Sun, H. 2018. Occurrence and
807 Phase Distribution of Neutral and Ionizable Per- and Polyfluoroalkyl Substances (PFASs) in the
808 Atmosphere and Plant Leaves around Landfills: A Case Study in Tianjin, China. Environ Sci
809 Technol 52(3), 1301-1310.
810 Trang, B., Li, Y., Xue, X.-S., Ateia, M., Houk, K. and Dichtel, W.R. 2022. Low-temperature
811 mineralization of perfluorocarboxylic acids. Science 377(6608), 839-845.
812 UN Environment Programme, 2020. Ninth Meeting of the Conference of the Parties to the Stockholm
813 Convention.
814 http://www.pops.int/TheConvention/ConferenceoftheParties/Meetings/COP9/tabid/7521/Defa
815 ult.aspx (Accessed 29th Feb 2023).

U.S. Environmental Protection Agency, 2016. Drinking water health advisory for perfluorooctanoic acid (PFOA). https://www.epa.gov/sites/production/files/2016-05/documents/pfoa_health_advisory_final-plain.pdf (Accessed 29th May 2023).

Wang, J., Pan, Y., Wei, X. and Dai, J. 2020a. Temporal trends in prenatal exposure (1998–2018) to emerging and legacy per-and polyfluoroalkyl substances (PFASs) in cord plasma from the Beijing Cord Blood Bank, China. Environmental Science & Technology 54(20), 12850-12859.

Wang, Q., Ruan, Y., Zhao, Z., Zhang, L., Hua, X., Jin, L., Chen, H., Wang, Y., Yao, Y. and Lam, P.K., 2022a. Per-and polyfluoroalkyl substances (PFAS) in the Three-North Shelter Forest in northern China: First survey on the effects of forests on the behavior of PFAS. Journal of Hazardous Materials 427, 128157.

Wang, S., Lin, X., Li, Q., Li, Y., Yamazaki, E., Yamashita, N. and Wang, X. 2022b. Particle size distribution, wet deposition and scavenging effect of per-and polyfluoroalkyl substances (PFASs) in the atmosphere from a subtropical city of China. Science of The Total Environment 823, 153528.

Wang, T., Wang, P., Meng, J., Liu, S., Lu, Y., Khim, J.S. and Giesy, J.P. 2015. A review of sources, multimedia distribution and health risks of perfluoroalkyl acids (PFAAs) in China. Chemosphere 129, 87-99.

Wang, W., Maimaiti, A., Shi, H., Wu, R., Wang, R., Li, Z., Qi, D., Yu, G. and Deng, S. 2019. Adsorption behavior and mechanism of emerging perfluoro-2-propoxypropanoic acid (GenX) on activated carbons and resins. Chemical Engineering Journal 364, 132-138.

Wang, W., Rhodes, G., Ge, J., Yu, X. and Li, H. 2020b. Uptake and accumulation of per- and polyfluoroalkyl substances in plants. Chemosphere 261, 127584.

Wang, Z., Cousins, I.T., Scheringer, M., Buck, R.C. and Hungerbühler, K. 2014. Global emission inventories for C4–C14 perfluoroalkyl carboxylic acid (PFCA) homologues from 1951 to 2030, Part I: production and emissions from quantifiable sources. Environment International, 62-75.

Wang, Z., DeWitt, J.C., Higgins, C.P. and Cousins, I.T. 2017. A never-ending story of per- and polyfluoroalkyl substances (PFASs)? Environmental Science & Technology 51(5), 2508-2518.

Wen, B., Pan, Y., Shi, X., Zhang, H., Hu, X., Huang, H., Lv, J. and Zhang, S. 2018. Behavior of N-ethyl perfluorooctane sulfonamido acetic acid (N-EtFOSAA) in biosolids amended soil-plant microcosms of seven plant species: Accumulation and degradation. Science of the Total Environment 642, 366-373.

Xiao, F. 2017. Emerging poly- and perfluoroalkyl substances in the aquatic environment: A review of current literature. Water Research 124, 482-495.

Xiao, F., Halbach, T.R., Simcik, M.F. and Gulliver, J.S. 2012. Input characterization of perfluoroalkyl substances in wastewater treatment plants: source discrimination by exploratory data analysis. Water Research 46(9), 3101-3109.

Xiao, F., Hanson, R.A., Golovko, S.A., Golovko, M.Y. and Arnold, W.A. 2018. PFOA and PFOS are generated from zwitterionic and cationic precursor compounds during water disinfection with chlorine or ozone. Environmental Science & Technology Letters 5(6), 382-388.

Xiao, F., Sasi, P.C., Alinezhad, A., Golovko, S.A., Golovko, M.Y. and Spoto, A. 2021. Thermal decomposition of anionic, zwitterionic, and cationic polyfluoroalkyl substances in aqueous film-forming foams. Environmental Science & Technology 55(14), 9885-9894.

Yamazaki, E., Eun, H., Taniyasu, S., Sakamoto, T., Hanari, N., Inui, H., Wu, R., Lin, H., Lam, P.K. and Falandysz, J. 2023. Residue Distribution and Daily Exposure of Per-and Polyfluoroalkyl Substances in Indica and Japonica Rice. Environmental Science & Technology.

Yang, Y., 2018. Chinese Food Composition Tables Standard Edition (in Chinese), Peking University Medical Press: Beijing, China.

Yu, P.F., Li, Y.W., Zou, L.J., Liu, B.L., Xiang, L., Zhao, H.-M., Li, H., Cai, Q.Y., Hou, X.W. and Mo, C.H. 2021. Variety-selective rhizospheric activation, uptake, and subcellular distribution of perfluorooctanesulfonate (PFOS) in lettuce (Lactuca sativa L.). Environmental Science & Technology 55(13), 8730-8741.

Zheng, G., Schreder, E., Dempsey, J.C., Uding, N., Chu, V., Andres, G., Sathyanarayana, S. and Salamova, A. 2021. Per-and polyfluoroalkyl substances (PFAS) in breast milk: Concerning trends for current-use PFAS. Environmental Science & Technology 55(11), 7510-7520.

Zhi, Y., Lu, H., Grieger, K.D., Munoz, G., Li, W., Wang, X., He, Q. and Qian, S. 2022. Bioaccumulation and translocation of 6:2 fluorotelomer sulfonate, GenX, and perfluoroalkyl acids by urban spontaneous plants. ACS ES&T Engineering 2(7), 1169-1178.

Zhou, J., Li, M., Li, J., Shao, Z., Liu, Y., Wang, T. and Zhu, L. 2020. Bioavailability and bioaccumulation of 6:2 fluorotelomer sulfonate, 6:2 chlorinated polyfluoroalkyl ether sulfonates, and perfluorophosphinates in a soil-plant system. Journal of Agricultural and Food Chemistry 68(15), 4325-4334.

Zhou, J., Li, S., Liang, X., Feng, X., Wang, T., Li, Z. and Zhu, L. 2021. First report on the sources, vertical distribution and human health risks of legacy and novel per-and polyfluoroalkyl substances in groundwater from the Loess Plateau, China. Journal of Hazardous Materials 404, 124134.

Zhou, J., Zhao, G., Li, M., Li, J., Liang, X., Yang, X., Guo, J., Wang, T. and Zhu, L. 2022. Three-dimensional spatial distribution of legacy and novel poly/perfluoroalkyl substances in the

883 Tibetan Plateau soil: Implications for transport and sources. Environment International 158,
884 107007.